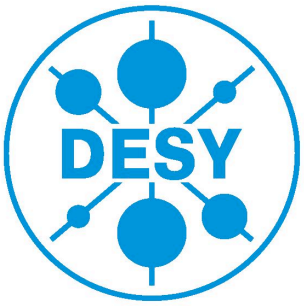

Tuning of Gluon Distribution Function at small-x via Pseudorapidity Distribution obtained from CMS and TOTEM detector

Krai Cheamsawat
Chulalongkorn University, Bangkok, Thailand
DESY summer student, CMS Group

Abstract

We have explored the problem of inconsistency between pseudorapidity distribution of charged particle in proton-proton collision whose data obtained from CMS and TOTEM detector and which obtained from simulation with various Monte-Carlo event generators. The objective of this work is to modify Parton Distribution Function(PDF) that describe the distribution of Gluon(Quark and Gluon are collectively called Parton) at various momentum fraction of protons in colliding beams. In this work we initially used data obtained from CMS and TOTEM detector to modify Parton Distribution Function. We found that value of gluon distribution at small momentum fraction crucial for tuning of Monte-Carlo event generator to give consistent result between simulation and experiment.

Acknowledgement

First, I would like to thank Hannes Jung, my supervisor who is very kind to all of his students for giving me many useful advices about the project and taking care of me throughout DESY summer student program. Next,I would like to thank Vardan Khachatyran, my co-supervisor who always fix my problems about programming in my progression of this project and sharing his experience of researching in high energy physics with me.

I also appreciate the kindness of Ph.D students who working in the same office as mine, Paolo Gunnellini who always share his snacks and make me laugh everytime, Samantha Dooling who always help me anytime I need without any excuses and Tomasz Fruboes, who is very experienced in computer stuffs.

Indispensably, I would like to thank National Science and Technology Development Agency(NSTDA) of Thailand for providing me a support for joining DESY summer student program.

Contents

1 Introduction

Although this work is mainly related to two issues: Monte Carlo event generators and Parton Distribution Function(henceforth we will briefly call it "PDF"), some more issues of high energy physics are still have to investigated in more details e.g. particle collider, particle detector, Quantum Chromodynamics(QCD) and Parton model.

1.1 Monte Carlo event generator

Monte-Carlo event generator is the indispensable tool for the study of High Energy Physics. By setting required environments of particle collision events that could be carried out in the real world by particle colliders, one can simulate such events in computer then obtain the result to compare with real experimental results that could lead to new discoveries.

In real world, studying particle physics is full of calculations and setting parameters for particles collisions such as luminosity, number of events, scattering amplitude, scattering cross section, decay rate, loop correction, angular distribution of final state particles and etc. Although we have handful of tools to study it, we are still lack of computing power to do the calculation to analyse the results from particle collisions that really happened in colliders. From this reason, it is unavoidable to take computer to our consideration as a tool to help us calculate these quantities.

Luckily, particle physics is involved with physics in the quantum scale. According to the probabilistic nature of Quantum Mechanics, we can somehow program a computer to generate the collision events by random process which is called Monte Carlo method. By adopting Monte Carlo method with event generator that is the large library of program, one can have Monte Carlo event generators for many purposes in study of particle physics.

In this work, we pay our attention to PYTHIA, Monte Carlo generator that is regularly used for simulation of proton-proton(antiproton) collision. It is increasingly important in LHC era because proton beam is used as colliding beam in LHC at CERN and PYTHIA consists of many features that suitable for generating hadronic collisions e.g. hard and soft interactions, parton distribution, initial/final-state radiations, parton showers, multiparton interactions, fragmentation and decay.

1.2 CMS & TOTEM experiment

As mentioned before, the main part of this work is done by comparing the simulated results from PYTHIA with experimental result obtained from data of final-state charged particles detected by CMS and TOTEM detector together. Data points we used in this work are pseudorapidity distribution of charged particles in both central and forward region from measurements of these two detectors.

1.2.1 CMS experiment

Compact Muon Solenoid(CMS) experiment is one of the largest particle detector complexes at CERN, it's located at the interaction point:IP5 of LHC ring underground of Cessy in France. CMS is 21.6 metres long, 15 metres in diameter, and weighs about 12,500 tonnes. It is multipurpose particle detector that can be used for searching and studying in many area of high energy physics such as Higgs boson, Dark Matter, Extra dimensions, Supersymmetry, etc.

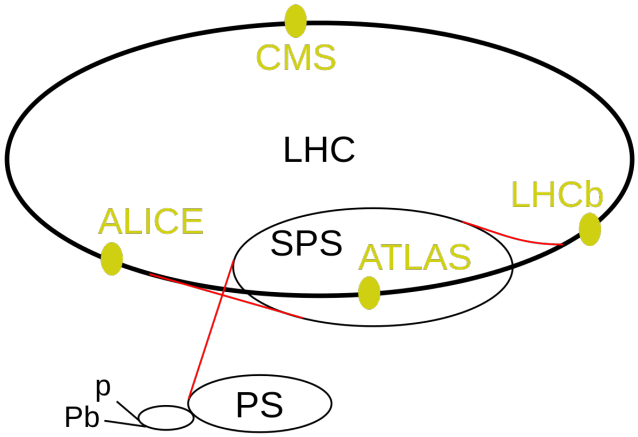

Figure 1.1: simplified map of LHC, large detector complexes(CMS, ATLAS, LHCb, ALICE) are located at each interaction point along LHC ring.

CMS is very effective for exploring wide range of physics because it consists of many layers of particle detectors with different characters throughout its cylindrical shape. These detectors are:

1. **The tracker**
   This layer is installed with many layers of silicon detectors that are used to record tracks of particles after interactions at the interaction point. It helps acquire the data of particle's momentum and charge. Data collected from this layer can also be used to reconstruct path of particle with high resolution.

2. **Electromagnetic Calorimeter**
   This layer of detector is designed to measure the energies of electrons and photons. Electromagnetic Calorimeter(ECAL) is made of crystals of Lead tungstate,$PbWO_4$ and because electrons and photons are very sensitive to electromagnetic interaction, when they pass through the matter, electron and photons will be easily lose their energies during their travelling in this layer. These energies from particles are then produce light in proportion to the particle's energy in very short time. This "scintillation" process helps amplify the signal of particle and measure its energy.

3. **Hadronic Calorimeter**
   The Hadronic Calorimeter(HCAL) is consist of layer of thick material which measure the energy of hadrons(i.e. protons, pions, kaons etc.), particle that composed of quarks and gluons. This layer of detector is very useful for measuring energy and number of charged hadronic final state which is the most abundant type of final state in proton-proton collision. These hardens usually come from hadronisation process of QCD.

4. **The magnet**
   The magnet of CMS is so powerful, it can be operated at maximum magnetic field of 4 Tesla which is very strong value of magnetic field. It is used to measure momentum of very high energy particles by measuring the radius of curvature of particle's path. Another use of this magnet is to bend the path of muons to muon detectors which placed in the outermost layer. These high intensity of magnetic field in CMS is produced by large superconducting solenoid which is fed by very cool liquid Helium for heat transferring purpose.

5. **Muon detectors and return yoke**
   This layer of CMS is very important for measuring many significant signals that reveal the unknown physics behind all measured signals. Muons can give a very clear signature for some events because muons are directly associated with electromagnetic interaction and weak interaction which associated to many kinds of particles. These muons are usually come out to be the final state of many collision events because muon is very stable particle so it can contribute to large proportion of signal and it doesn't lose its energy rapidly in electromagnetic calorimeter like electrons and photons so they usually pass through inner layer of detector with high energy. This muon detectors layer is consists of three kinds of detectors: drift tubes, cathode strip chamber and resistive plate chambers. By using these detector altogether with return yoke which are layers of iron that providing a high intensity of magnetic field; energy, momentum and path of muon can be measured with high precision.

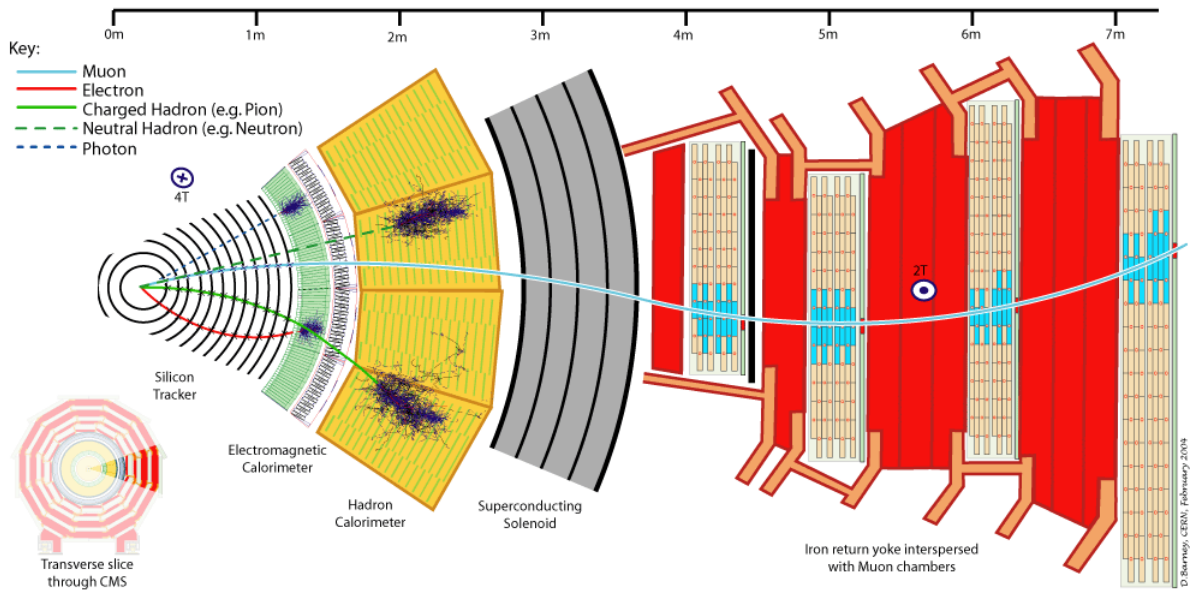

Figure 1.2: cross sectioned view of CMS, it shows all layers of CMS detector

1.2.2 TOTEM experiment

When proton scattered with proton in the collider, there are two main types of scattering processes: elastic and inelastic scattering. Elastic scattering is simple, in which proton scattered with proton without any breaking of either protons into other different final states. Inelastic scattering is very nontrivial, there can be many process such as soft processes, hard processes, single diffractive or non single diffractive processes, etc. It also produce many topologies of final states. In addition, physics of diffractive scattering is not fully understood until now because it involved in non-perturbative QCD where perturbative approach is unreliable. Therefore, measurement of total cross section and diffractive cross section is very important for making more understanding of nature of proton-proton collision. Because of requirement to study in more details of total cross section, the "Total elastic and diffractive cross-section measurement"(TOTEM) experiment was then designed and installed at two ends of CMS detector to measure scattered particles in forward region(pseudorapidity range: 3.0-7.0) to complement with data from CMS detector which make a measurement in central region(pseudorapidity range: 0.0-3.0).

TOTEM experiment consists of three detector areas: Roman Pots, T1 telescope and T2 telescope.

- Roman Pots detectors are used for detection of scattered proton in forward region from elastic and inelastic scattering. They are placed at 147 and 220 meters away from interaction point along the beam pipe in both forward and backward directions with the full azimuthal detection area.

- T1 telescope is used to detect scattered particle from inelastic scattering in pseudorapidity range between 3.1-4.7. Two arms of T1 telescope are installed at ±9 meters from interaction point.
- T2 telescope is used to detect scattered particle from inelastic scattering in pseudorapidity range between 5.3-6.5. It is Gas Electron Multipliers(GEM) detector which gives a good resolution of particle's position.Two arms of T2 telescope are installed at ±13.5 meters from interaction point.

Figure 1.3: CMS and TOTEM detector. Notice the very narrow angular region covered by T1 and T2 telescope.

1.3 The problem with $\frac{dN_{ch}}{d\eta}$ distribution

Pseudorapidity distribution is a distribution that tell how many particles are scattered to different angle relative to the direction of beam pipe. The significant feature of pseudorapidity distribution is when the energy of particle be much larger than its mass or case of massless particle, pseudorapidity distribution will be a Lorentz invariance distribution. This means that we will get the same shape of pseudorapidity distribution as long as we observe the collision event in reference frames which among them are related by boosting along the beam pipe(or $\pm z$ direction).

pseudorapidity(η) is defined by:

$$\eta = -\ln\left(\tan\frac{\theta}{2}\right) \tag{1.1}$$

where θ is the angle of particle's momentum relative to direction of beam.

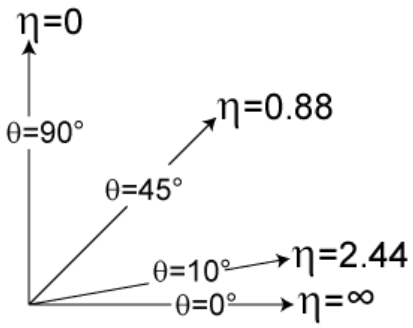

Figure 1.4: Some values of η and their corresponding θ.

Pseudorapidity is introduced, so we can now say about central and forward region in the context of high energy physics experiments. In this work, our data of pseudorapidity distribution are taken from CMS and TOTEM experiment, the former is for measurement in central region, the latter is for measurement in forward region.

In the context of this work, central region is the angular region in which $|\eta| \approx 0.0 - 2.2$ and forward region in which $|\eta| \approx 5.3 - 6.5$.

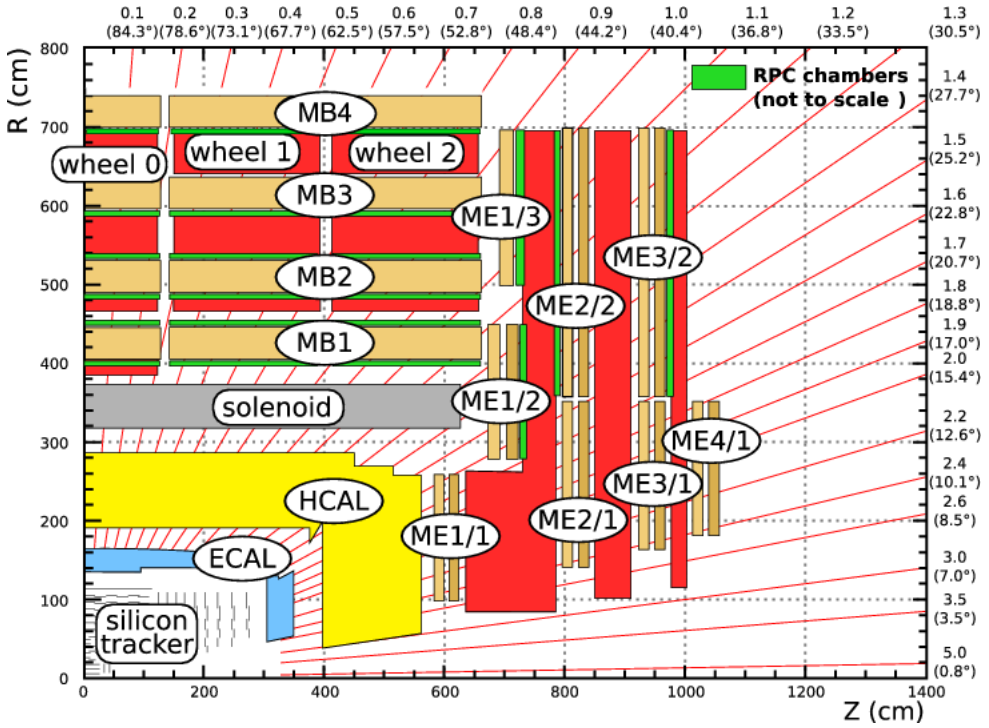

Figure 1.5: Pseudorapidity region of CMS tracker is $|\eta| = 0.0 - 2.5$ and for CMS calorimeter is $-6.6 < \eta < 5.2$.

Measurement of pseudorapidity distribution from CMS & TOTEM in July 2012 LHC run [1] is done with three topologies of final state event selection:

- Inclusive sample where there is at least one primary track triggered in one or both T2 telescopes.
- Non-single diffractive(NSD)-enhanced sample which requiring at least one primary track in both T2 telescopes.
- Single diffractive(SD) dissociation-enhanced sample, the event sample in which at least one primary track is reconstructed in one T2 telescope.

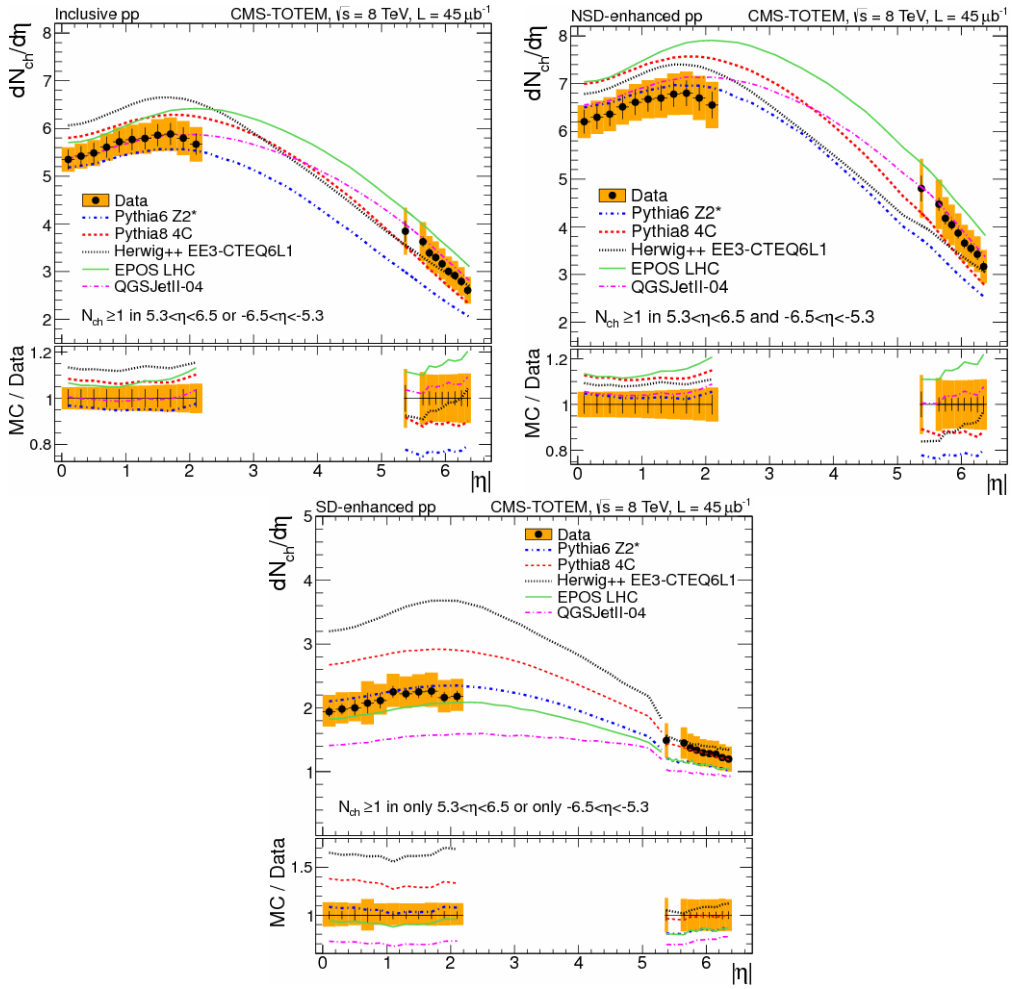

Figure 1.6: Charged-particle pseudorapidity distribution from inclusive sample(left), NSD sample(middle) and SD sample(right). The measurements are compared with PYTHIA6 tune Z2, PYTHIA8 tune 4C, HERWIG++ tune EE3-CTEQ6L1, EPOS tune LHC and QGSJetII-04 Monte Carlo generators

From Figure 1.6, disagreement between data and simulation from MC generator is shown, none of these MC generators gives consistent result with data. This discrepancy leads to question about the difference among these MC generators and their tunes. Each tune of MC generator differ in many way in its default setting e.g. hadronisation model, model for diffractive process, Parton Distribution Function(PDF) etc.

1.4 Parton Distribution Function

Before QCD was firmly established, the fundamental theory of strong interaction had been approached in many ways. One of approaches that still work well until now is Parton model. It was proposed by Richard P. Feynman in 1969 as a way to analyse the data from hadronic collision at high energy. Hadron in the viewpoint of Parton model is composite particle which consists of point-like constituents called "Partons". When these hadrons is observed in "infinite momentum frame" where its momentum be very high (this approximation is valid in high energy regime) says, P, the momentum of hadron will be shared to each parton by the fraction "x". Then summation of all parton's momentum could roughly looks like:

$$\sum_{i \in hadron} x_i P = P \tag{1.2}$$

The experimental verification of Parton model was first achieved by Deep Inelastic Scattering(DIS), in which high energy lepton(electron or sometimes neutrino) is scattered with hadron(usually proton). When minus of momentum transfer squared ($Q^2 = -q^2$) of exchange boson(γ or Z for neutral current and $W^{\pm}$ for charged current) is high, it can "knock" hadron apart into Partons. These Partons then develop an unobserved hadronic final state X whose mass is $M_X^2 = (p+q)^2 \geq M^2$ where p is four-momentum of hadron, q is four-momentum of exchange boson and M is mass of hadron.

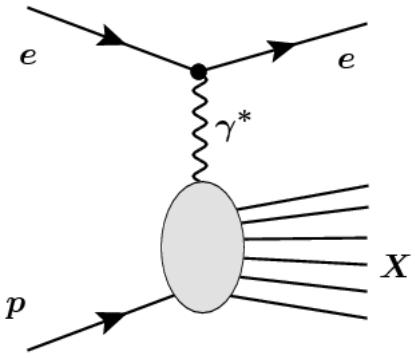

Figure 1.7: Feynman diagram illustrating the $e + p \rightarrow e + X$ DIS.

Scattering amplitude of Feynman diagram in Figure 1.7 can be computed in context of Parton model to obtain measurable differential cross section of the process. What

can be extracted from cross section measurement are structure functions that describe the structure of hadron. In the QCD-improved Parton model which has been modified by the concept of quarks and gluons. Structure functions of proton when probed by electron are:

$$F_2(x, Q^2) = x \sum_i e_i^2 q_i(x) \tag{1.3}$$

$$F_1(x, Q^2) = 2xF_2(x, Q^2) \tag{1.4}$$

where $q_i(x)$ is Parton Distribution Function(PDF) of i-flavour quark, e_i is electric charge(in unit of proton charge) of i-flavour quark.

Physical meaning of PDF is the probability density of finding parton in momentum fraction x and $q_i(x)dx$ is the probability to found parton of flavour i in the momentum fraction interval x to $x + dx$.

Recall eqn.(1.2), the precise momentum sum rule of PDF is then:

$$\int_0^1 \sum_i x q_i(x) dx = 1 \tag{1.5}$$

But the relation in eqn.(1.5) is not true when we take only valence quark(e.g valence quark content of proton is uud) into account. Let's recall that in infinite momentum frame where proton's momentum is very high, the effect of time dilation can be large enough for observer outside the proton to "see" the sea of quark and gluon emerged from interaction among valence quarks. Then, PDF for each quark should be modified to be:

$$q_i(x) = q_i^V(x) + \bar{q}(x) \tag{1.6}$$

where $q_i^V(x)$ is PDF of valence quark and $\bar{q}(x)$ is PDF of sea(anti) quark.
Nevertheless, the contribution from quarks alone is not enough. Hadron's momentum is also carried by gluon, hence one need to introduce another PDF which is PDF of gluon $g(x)$. Then, the actual momentum sum rule for hadron is:

$$\int_0^1 x[\sum_i q_i(x) + g(x)]dx = 1 \tag{1.7}$$

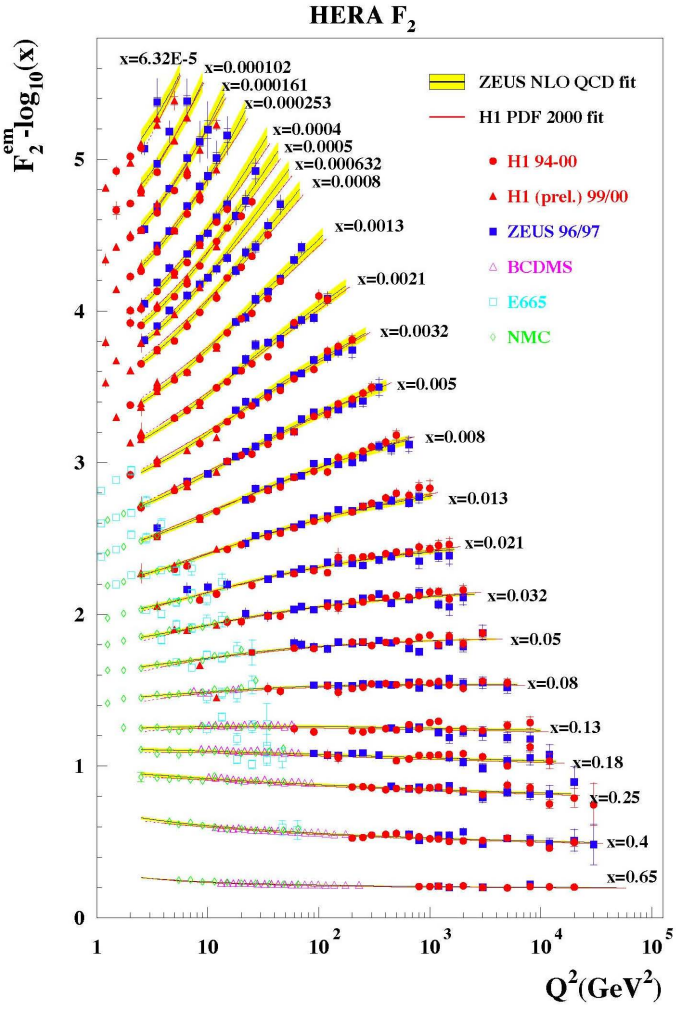

Figure 1.8: Structure function $F_2(x, Q^2)$ determined by combined data from H1, ZEUS, BCDMS, E665 and NMC

2 PDF in Monte Carlo generator and the way to resolve $\frac{dN_{ch}}{d\eta}$ problem

As already stated in section 1.3 that default setting are different in each tune of MC generator. One of these settings is PDF that could make the difference among MC generators and measurement.

2.1 Variation of Gluon Distribution Function

The study of QCD in low energy scale is very complicated by mean of calculation and unclear physical picture due to the nontrivial nature of QCD at low energy scale in which non-perturbative effect plays a major role, perturbation theory can no longer apply to QCD at low energy or momentum scale.

The figure below shows the running coupling constant of QCD. At lower energy scale, coupling constant becomes larger. This means that perturbation theory that always work in the limit $\alpha_s(Q) \ll 1$ will be broken down at low energy scale of QCD.

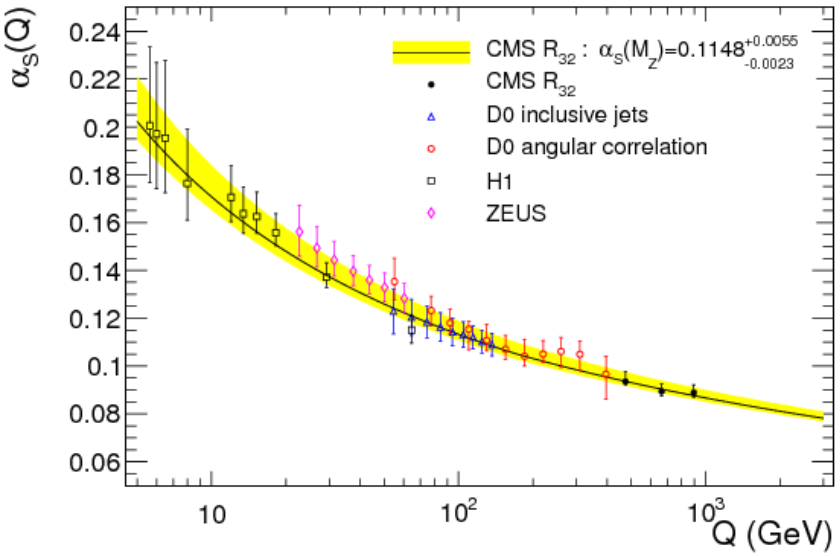

Figure 2.1: Data from many experiments confirm the running coupling constant of QCD at different momentum scale

This nontrivial nature of QCD at low momentum scale leads to the uncertainty of PDF in different tune of MC generators. In each MC generator, the model and calculation schemes for simulation of collision events are different. For example, some of them may use LO(Leading order) calculation to calculate scattering amplitude of QCD processes to obtain PDF, while some of them may use NLO(Next to leading order) or NNLO calculations to calculate PDF instead. Furthermore, coupling constant at reference renormalisation scale may be different due to the model and calculation scheme that implemented to MC generator. This complexity results in the uncertainty of gluon distribution function at small-x region in many PDF profiles and default tunes of MC generators.

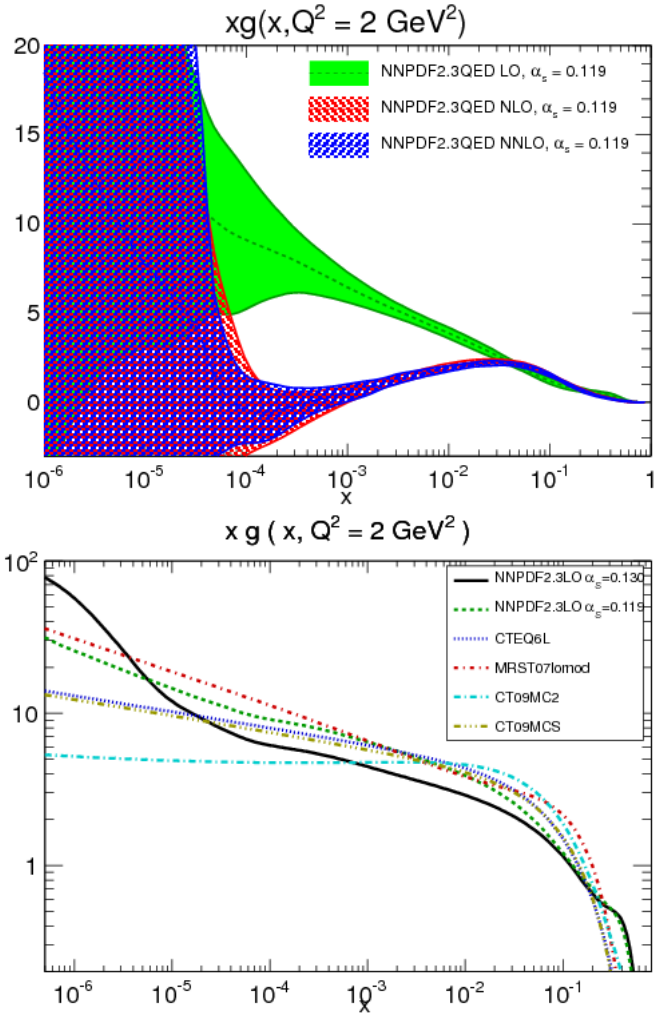

Figure 2.2: Gluon distribution function of NNPDF family(top) and some tunes of MC generators(bottom). Most of gluon distribution function are agreed with each other at x closed to 1 but very uncertain at small-x region. These figures are taken from Ref [3].

2.2 Tuning of PDF

In order to deal with the inconsistency of pseudorapidity distribution between simulation from MC generator and experiment. One way that we can do to solve is to modify gluon distribution function at small-x by adding some functions that could provide more contribution of gluon at small-x than original one.

One possible modified PDF is:

$$xg(x) \equiv f_1(x) = \left(p_2^3 \ln\left(\frac{p_1}{x}\right)\right)\left(\frac{1}{2} - \frac{1}{\pi}\arctan\left(a(x-p_1)\right)\right)^b + f(x) \tag{2.1}$$

where a and b are irrelevant constant, p_1 and p_2 are parameters of this PDF that will be used for tuning of MC generator to be agreed with experimental result.

shape of this function for some set of p_1 and p_2 is:

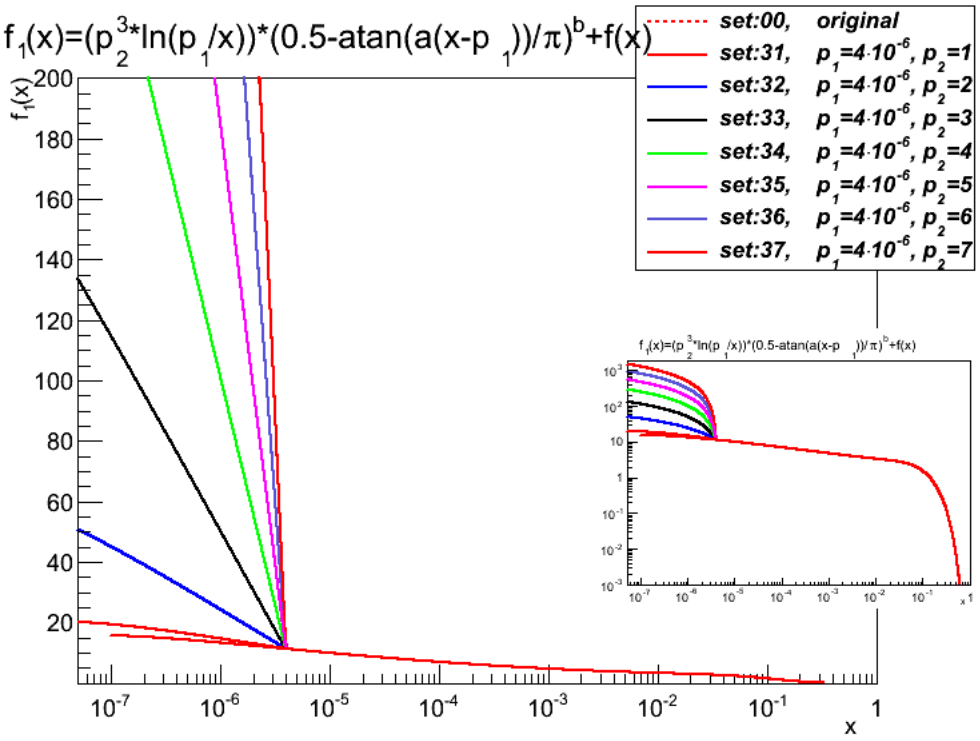

Figure 2.3: Example of modified PDF when $p_1 = 4 \times 10^{-6}$, $p_2 = 1, 2, 3, 4, 5, 6, 7$ the smaller one is shown in log scale in vertical axis

From figure 2.3 and eqn.(2.1), the modifying part of PDF is vanished at $x = p_1$ and very suppressed at $p_1 < x < 1$. Moreover, this function is very steep at $x < p_1$ especially when $p_2 \geq 1$.

One can see that p_1 is the starting point at which slope of PDF suddenly change to be very steep in small-x region and p_2 is effectively the slope of PDF in small-x region. So henceforth p_1 and p_2 will be namely called "starting point" and "slope" of PDF at small-x respectively. $f(x)$ is simply the modified PDF when both p_1 and p_2 are zero(i.e. the original one without any modification). So for later convenience, it will be called "set 00".

2.2.1 Implementation of PDF to MC generator

In this work, we've prepared 49 profiles of modified PDF by setting 49 different pairs of (p_1, p_2) values, then applied them to PYTHIA together with Rivet[1] analysis code to obtain pseudorapidity distribution and compare them with one obtained from CMS & TOTEM data [1].

values of p_1 and p_2 used in sample of PDF are:

number represented p_1	1	2	3	4	5	6	7
starting point	10^{-6}	2×10^{-6}	4×10^{-6}	6×10^{-6}	8×10^{-6}	10^{-5}	2×10^{-5}

number represented p_2	1	2	3	4	5	6	7
slope	1	2	3	4	5	6	7

Hence, number of modified PDF in sample are ordered to be:

$$(p_1, p_2) = \{(1,1), (1,2), ..., (1,7), (2,1), (2,2), ..., (7,6), (7,7)\}$$

Some of results are illustrated here

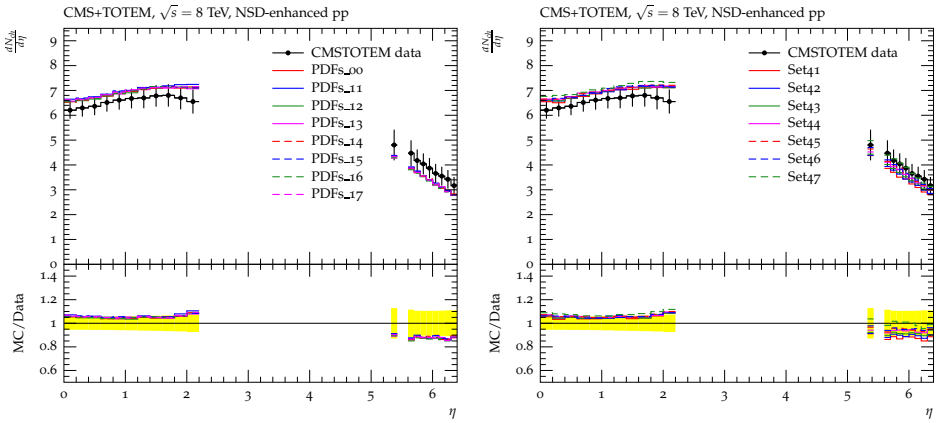

Figure 2.4: Pseudorapidity distribution in NSD-enhanced event selection obtained by implementing PDF (1,1),...,(1,7) and (4,1),...,(4,7). In the left figure, results from PDF 00 is shown.

[1] *Robust Independent Validation of Experiment and Theory*(Rivet) is a program used for validation of Monte Carlo generators.

2.2.2 Finding the "good" PDF

In order to choose the good PDFs out of the others, integral(i.e. area under pseudorapidity distribution) of each histogram obtained from each PDF are calculated separately to be one of central and forward region. Then taking ratio of these integrals to the integral obtained from set 00 to see their deviation from original PDF.

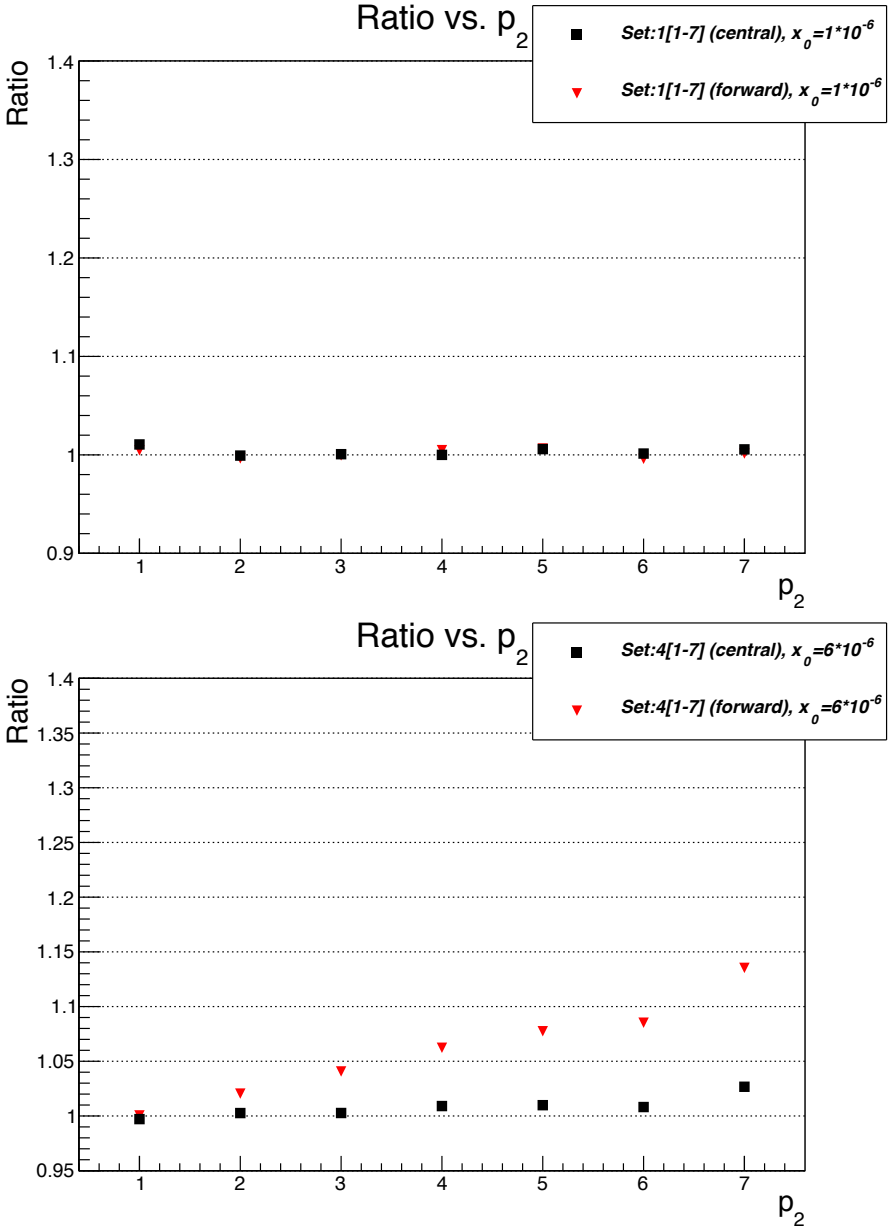

Figure 2.5: Example of graphs showing the ratio of integral of PDF (1,1),...,(1,7) (top graph) and (4,1),...,(4,7) (bottom graph) versus values of p_2. These graphs are ratios of integral in NSD-enhanced event selection corresponding to results shown in figure 2.4

3 Results & Discussions

3.1 Candidates of "good" PDF

After the procedure in previous section, by observing the the comparison of results from 49 PDF profiles with data points. Some of them are chosen to be candidates of "good" PDF that could be implemented to MC generator to simulate the reliable results compared with other measurements later on.

Collection of best out of other results are:

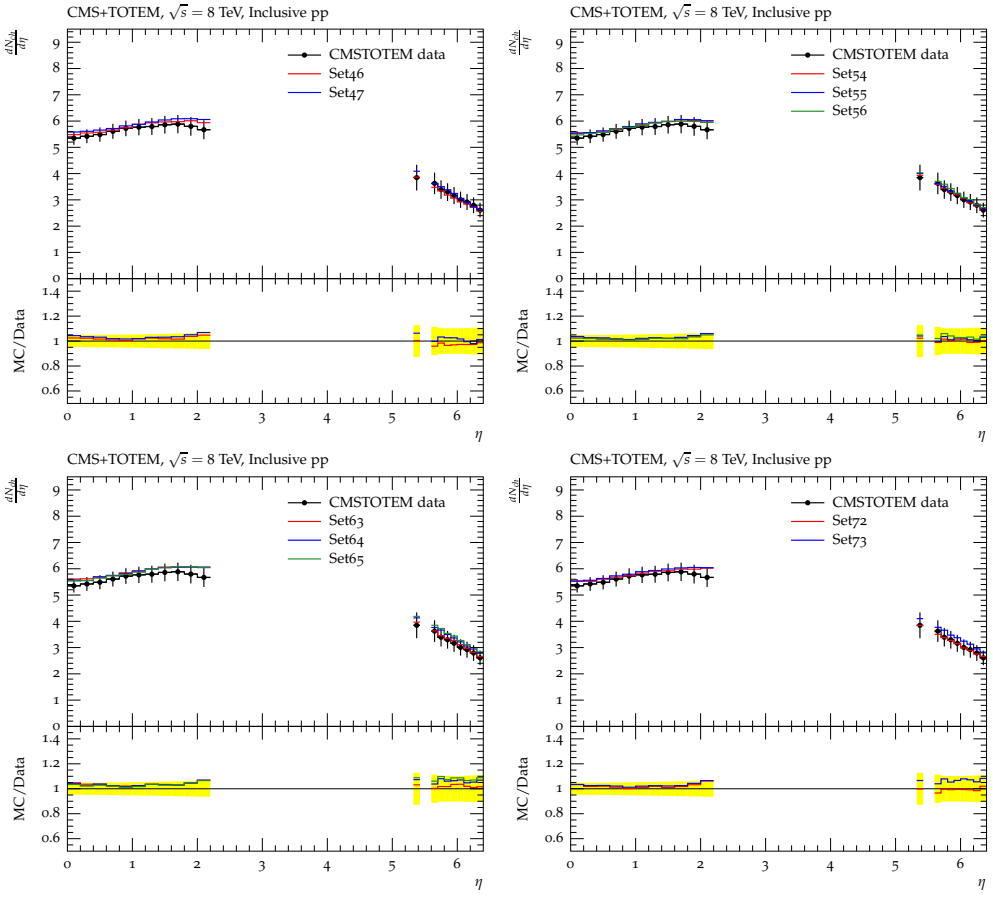

Figure 3.1: Good pseudorapidity distributions in inclusive event selection obtained from PDF in which $p_1 = 6 \times 10^{-6}$(upper left), 8×10^{-6}(upper right), 1×10^{-5}(lower left), 2×10^{-5}(lower right) respectively.

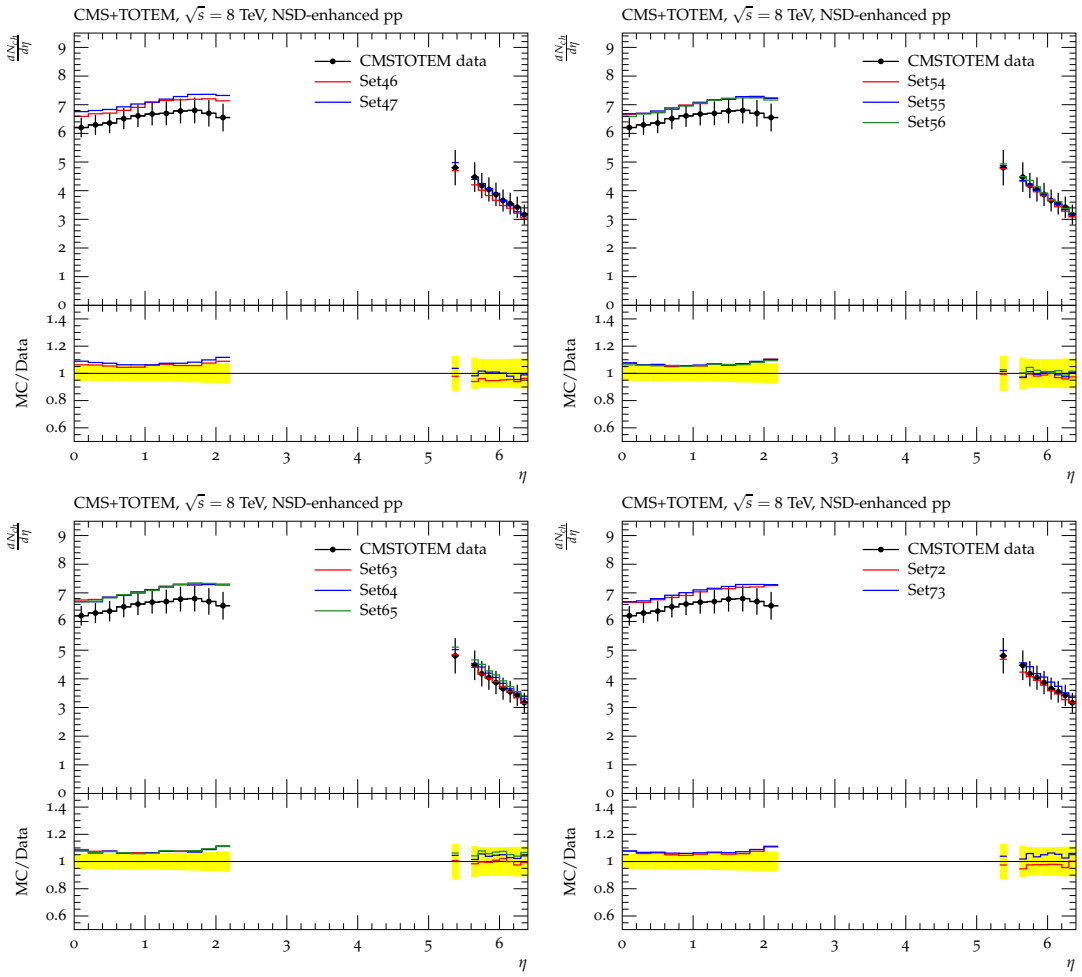

Figure 3.2: Good pseudorapidity distributions in NSD-enhanced event selection obtained from PDF in which $p_1 = 6 \times 10^{-6}$(upper left), 8×10^{-6}(upper right), 1×10^{-5}(lower left), 2×10^{-5}(lower right) respectively.

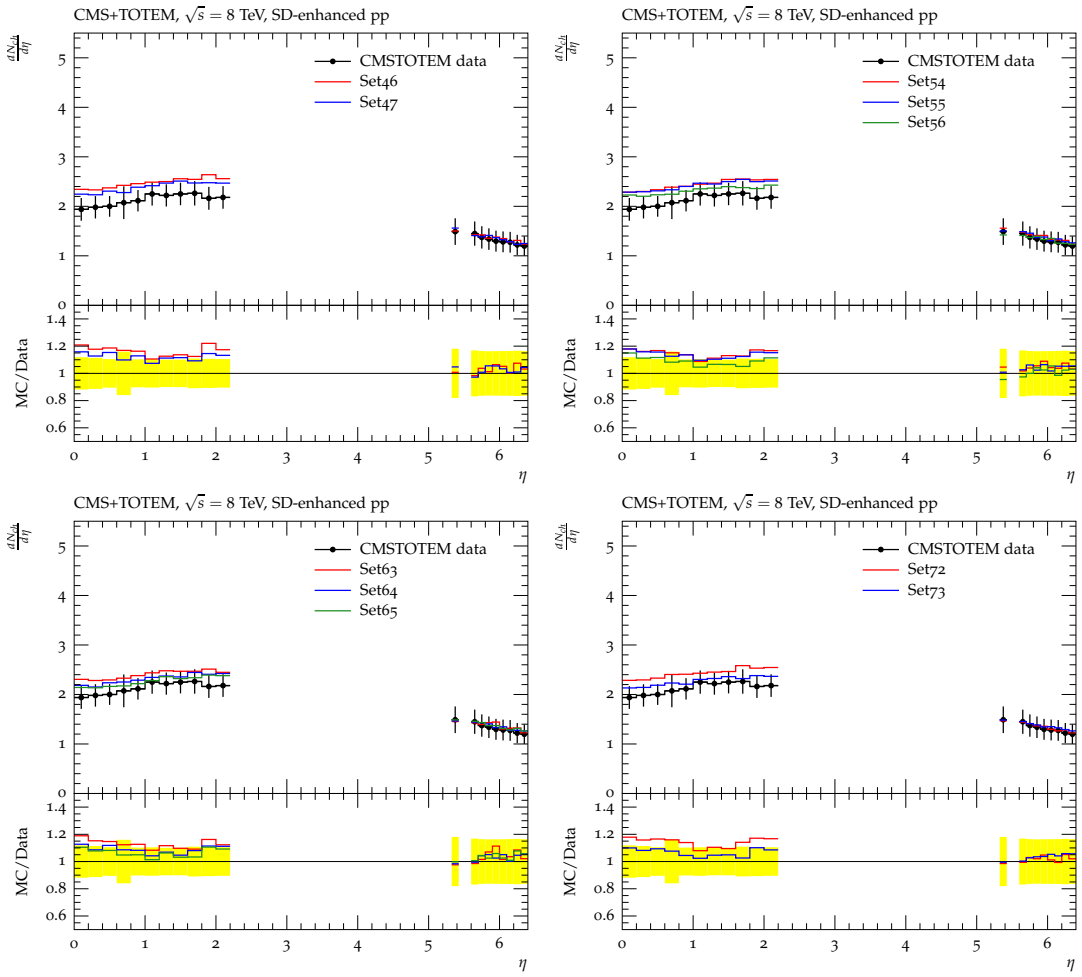

Figure 3.3: Good pseudorapidity distributions in SD-enhanced event selection obtained from PDF in which $p_1 = 6 \times 10^{-6}$(upper left), 8×10^{-6}(upper right), 1×10^{-5}(lower left), 2×10^{-5}(lower right) respectively.

From figure 3.1, 3.2, 3.2 in NSD and SD event selection, none of results gives a consistent distribution in central region although they give consistent result in forward region. Nevertheless, in inclusive event selection which is simply the union of NSD and SD set of event sample, these results are very well agreed with measurement.

The value of ratios from 49 pairs of (p_1, p_2) in NSD, SD and inclusive event selection are:

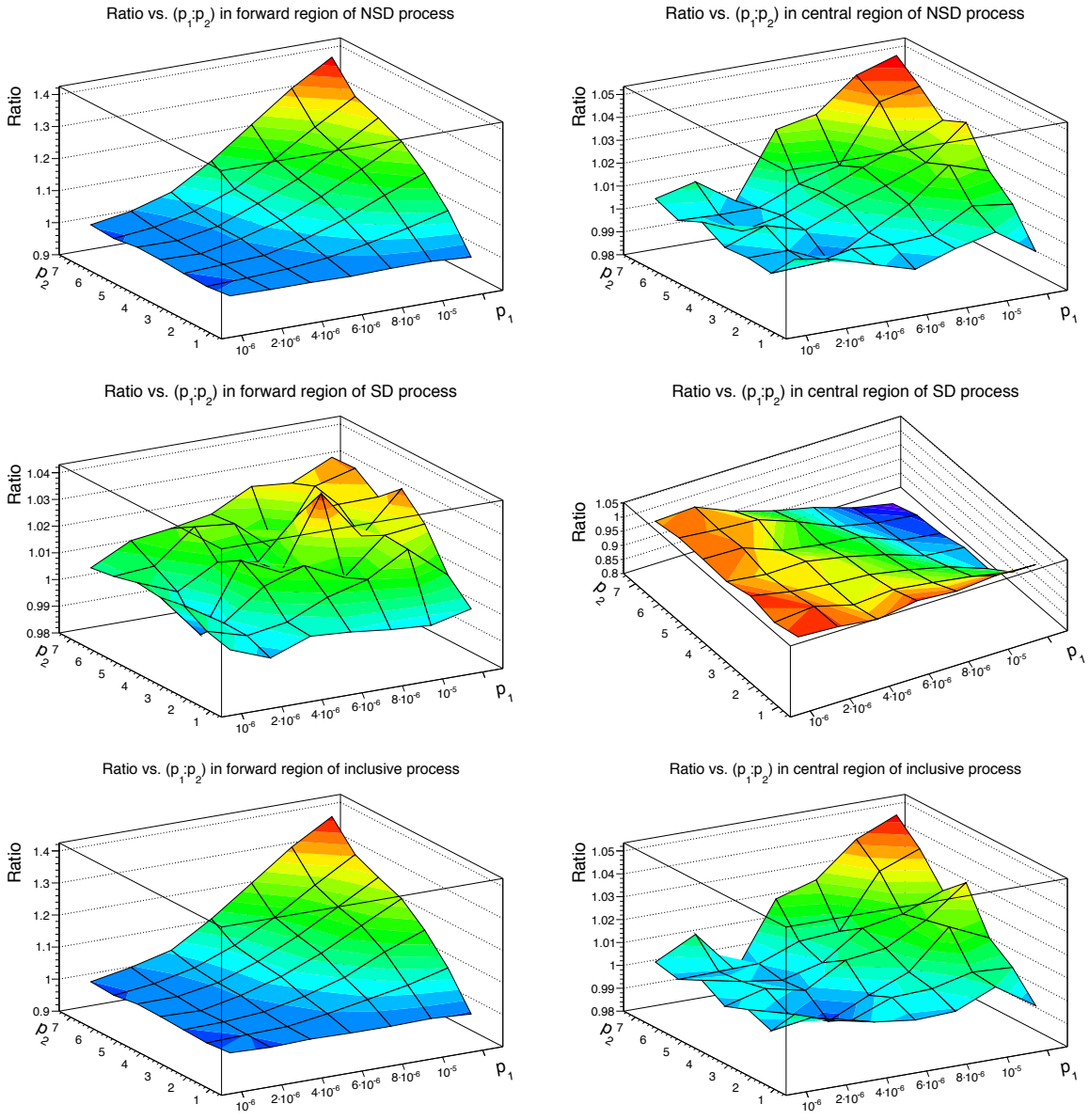

Figure 3.4: Surface plots of ratios of integral in domain of (p_1, p_2) values. This figure shows plots in three event sample: inclusive(top row), NSD-enhanced(middle row), SD-enhanced(bottom row). Left column and right column are for forward and central region respectively.

3.1.1 Common feature of good PDFs

In the finding, we found a feature that these good PDFs have in common, to see it clearly, these ratios of integrals should be observed in more detail.

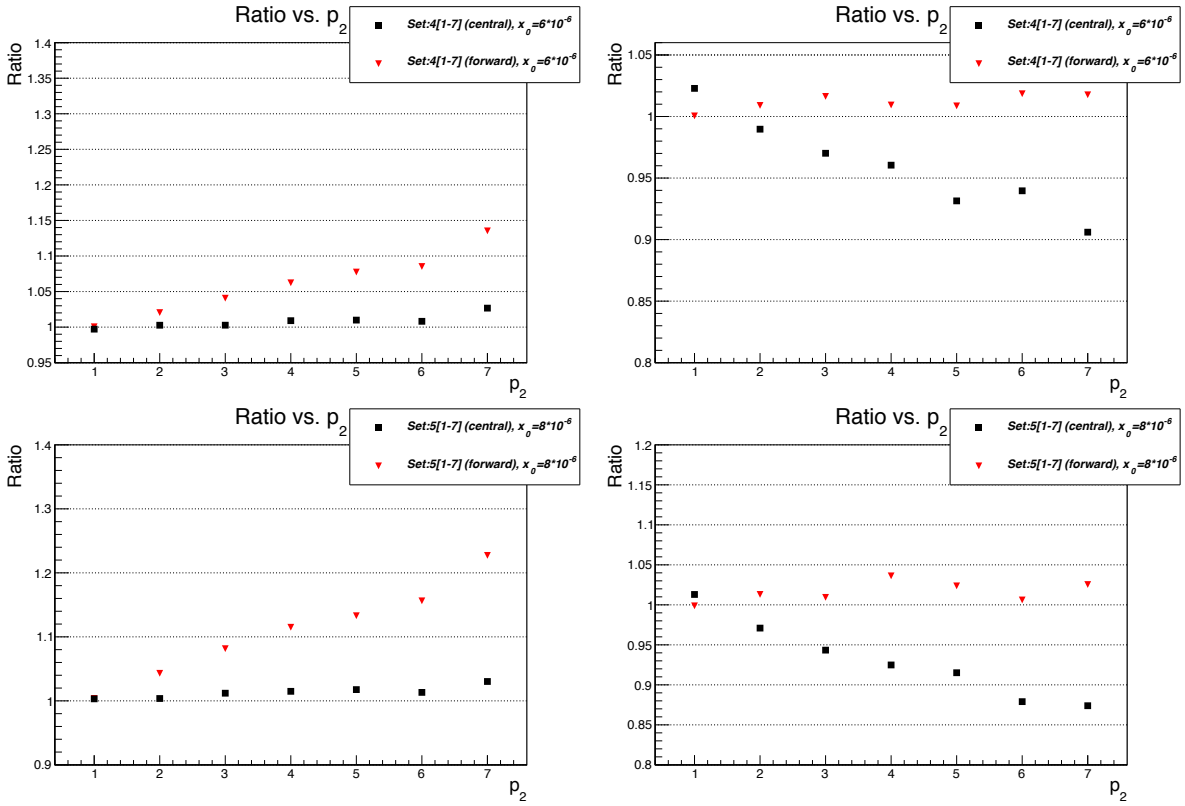

Figure 3.5: Two dimensional plot of ratios versus values of p_2 for PDF with $p_1 = 6 \times 10^{-6}, 8 \times 10^{-6}$. Left column and right column are for NSD and SD-enhanced event sample respectively.

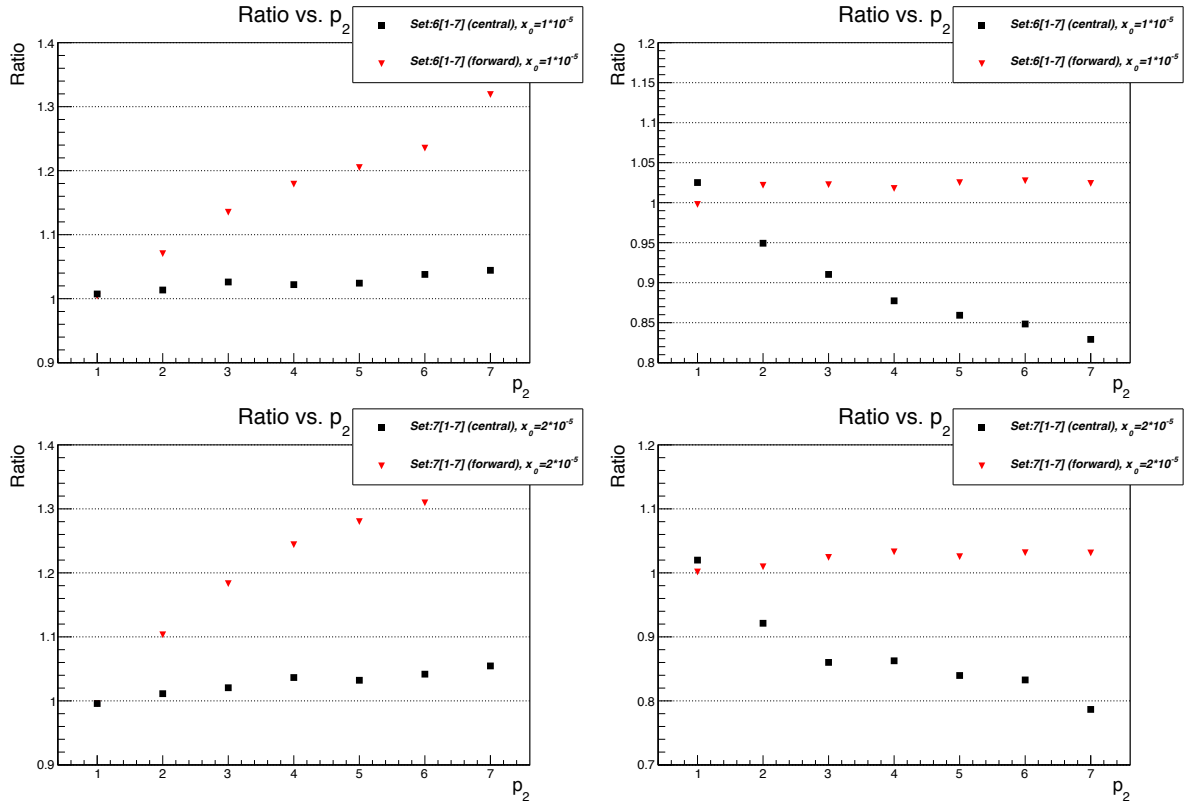

Figure 3.6: Two dimensional plot of ratios versus values of p_2 for PDF with $p_1 = 10^{-5}, 2\times 10^{-5}$. Left column and right column are for NSD and SD-enhanced event sample respectively.

The common feature of these good PDF profiles is the difference of ratio of integral between forward and central region are all approximately $0.1 - 0.15$, it can be shown symbolically as:

$$|r_{forward} - r_{central}| \approx 0.1 - 0.15$$

For each good PDF profile. Where $r_{forward}$ and $r_{central}$ are ratios in forward and central region respectively. This finding tell somethings about criteria to choose good PDF in this (toy)model.

3.2 Confirming the goodness of PDFs

Since these good PDFs have been chosen by comparing with result from measurement reported in Ref.[1] alone, in order to verify the validity of these good PDFs, we need to apply these PDFs with MC generator to simulate pseudorapidity in another setup of collision events to see if it agree with other measurements. We simulate pseudorapidity distribution by applying good PDFs to PYTHIA and compare the result with measurement from TOTEM experiment [2] in which they found that none of trial MC generators agree with the data.

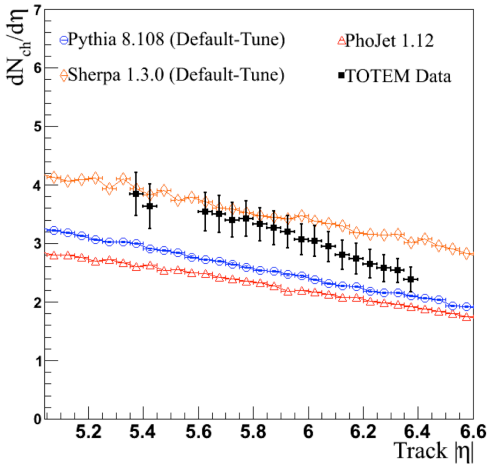

Figure 3.7: Result obtained in Ref.[2], none of MC generators can simulate pseudorapidity distribution that consistent with data points.

For our chosen good PDFs:

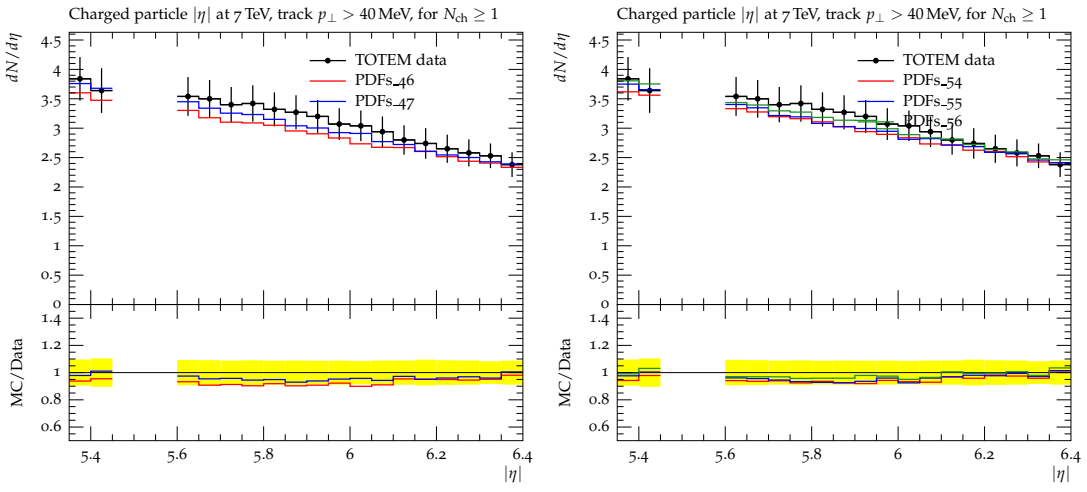

Figure 3.8: Pseudorapidity distribution obtained from "good" PDF: 46, 47 (left) and 54, 55, 56 (right) compared with data.

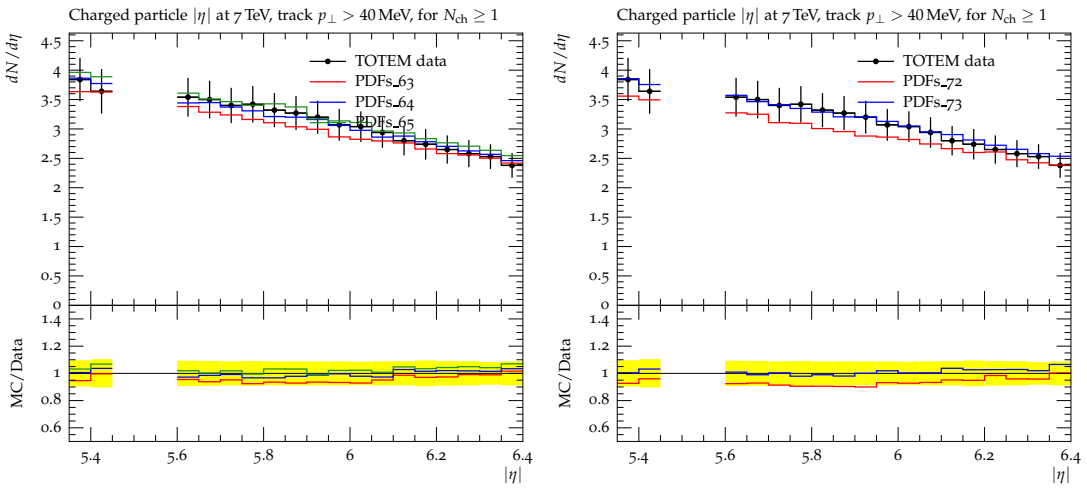

Figure 3.9: Pseudorapidity distribution obtained from "good" PDF: 63, 64, 65 (left) and 72, 73 (right) compared with data.

It can be clearly seen that all of our good PDFs give better compatibility(at least in forward region) than the result shown in figure 3.7.

3.3 More observation

From what previously mentioned in this chapter, one important fact about tuning of PDFs in order to get good PDFs that can give consistent result with measurement and reliable simulations when applying for future uses is both starting point of small-x region(p_1) and slope(p_2) should be tuned harmoniously to each other. That is to say, when slope become steeper, starting point should become smaller and vice versa. This leads to another observation about dependence between p_1 and p_2 in this model.

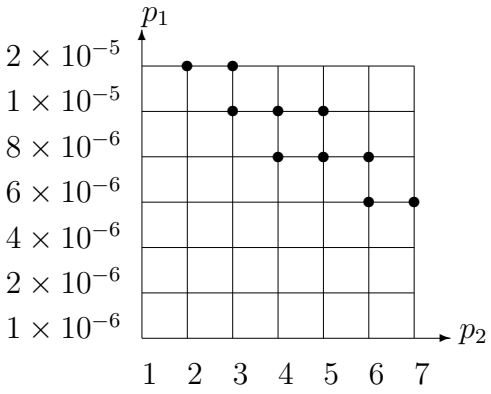

Figure 3.10: Position of good PDFs in (p_1, p_2) space.

From figure 3.10, there should be a relation between p_1 and p_2 that could be investigated outside the scope of this study.

4 Conclusions

Parton Distribution Function(PDF) is a distribution function that tell us about the probability to find partons(quarks and gluons) at any value of fraction(x) of hadron momentum. PDF is a crucial ingredient of Monte Carlo event generator, simulation of proton-proton collisions that presently conducted in many high energy particle accelerators are very dependent on the PDF used in each MC generator. This means that PDF is one factor that could define the reliability of MC generator when compare the simulation with experimental results.

Pseudorapidity distribution is the distribution that give the information about how number of final-state particle distribute in angular coordinate relative to the beam pipe of accelerator. In this work, we have tried to resolve the problem of inconsistency of pseudorapidity distribution obtained from applying default PDF that provided in MC generator and the distribution obtained from experimental data. Our trial is done by adding the modifying part to the original PDF and varying them with two parameters which are starting point of modification and slope of PDF at small-x region.

By implementing the sample of modified PDF within our range of parameters to MC generator then simulating pseudorapidity distribution to compare with data from CMS & TOTEM detector, we found that some of PDFs give an agreed result with the data within our acceptance. After confirming the validity of our chosen "good" PDF by applying them to simulation of pseudorapidity distribution and comparing these distributions with another data set from TOTEM, the conclusions of this work is the followings.

- Pseudorapidity distribution of charged particles in forward region of proton-proton collision is very sensitive to gluon distribution function at small-x region.
- Pseudorapidity distributions obtained from good PDF work very well in forward region but still lack of precision in central region. Therefore, we are still need further investigation for improvement of pseudorapidity distribution in central region.
- In this (toy)model, "both" the slope of PDF in small-x region(p_2) and the starting point(p_1) can improve the agreement between MC generator and measurement.

Nevertheless, the relation between p_1 and p_2 of good PDFs is needed to be investigated for more detail but it is out of scope of this study.

Bibliography

[1] S. Chatrchyan *et al.* [CMS and TOTEM Collaborations], "Measurement of pseudorapidity distributions of charged particles in proton-proton collisions at $\sqrt{s} = 8$ TeV by the CMS and TOTEM experiments," arXiv:1405.0722 [hep-ex].

[2] G. Antchev *et al.* [TOTEM Collaboration], "Measurement of the forward charged particle pseudorapidity density in pp collisions at $\sqrt{s} = 7$ TeV with the TOTEM experiment," Europhys. Lett. **98**, 31002 (2012) arXiv:1205.4105 [hep-ex].

[3] P. Skands, S. Carrazza and J. Rojo, "Tuning PYTHIA 8.1: the Monash 2013 Tune," arXiv:1404.5630 [hep-ph].

[4] F. D. Aaron *et al.* [H1 Collaboration], "Inclusive Measurement of Diffractive Deep-Inelastic Scattering at HERA," Eur. Phys. J. C **72**, 2074 (2012) [arXiv:1203.4495 [hep-ex].

[5] V. Barone and E. Predazzi, *High-Energy Particle Diffraction*, Springer-Verlag Berlin Heidelberg New York (2002)

[6] T. Cheng, L. Li, *Gauge Theory of Elementary Particle Physics*, Oxford University Press, 1985.

[7] R. K. Ellis, W. J. Stirling, B.R. Webber, *QCD and Collider Physics*, Camb. Monogr. Part. Phys. Nucl. Phys. Cosmol., 1996